Wave Tunneling and Hysteresis in Nonlinear Junctions

Wenjie Wan, Stefan Muenzel, and Jason W. Fleischer

Department of Electrical Engineering, Princeton University, Princeton, New Jersey 08544, USA
Princeton Institute for the Science and Technology of Materials, Princeton University, Princeton, New Jersey 08544, USA

(Received 11 March 2009; published 18 February 2010)

We consider the nonlinear tunneling of a plane wave through a small barrier potential in a medium with self-defocusing, or repulsive, interactions. We show that nonlinearity can either suppress or enhance transmission rates, determined by whether the initial kinetic energy is above or below the barrier height. Associated with this threshold is the appearance of two distinct hysteresis loops, going clockwise or counterclockwise, respectively. Spatial dynamics upon reflection and transmission reveals the formation of dispersive shock waves (dark soliton trains) due to phase jumps at the interfaces and wave steepening during propagation. The results are demonstrated experimentally for optical wave tunneling through a refractive index defect but will hold for any Schrödinger system that contains a nonlinear junction.

DOI: 10.1103/PhysRevLett.104.073903 PACS numbers: 42.65.Sf, 03.75.Lm, 47.37.+q

Wave tunneling at interfaces and through barriers is a fundamental and wide-ranging problem in physics. While the linear behavior is a textbook problem, the nonlinear case has received far less attention. Even for a single interface, nonlinearity can significantly modify the boundary conditions, leading to multivalued transmission rates [1,2]. For double interfaces, i.e., tunneling junctions [3–5], the problem is further complicated by the nonlinear dynamics between the faces [6,7]. Here, we exploit photorefractive optical systems to study nonlinear wave tunneling by small barrier potentials. We show numerically and experimentally that self-defocusing nonlinearity can greatly alter transmission, with either enhanced or suppressed rates possible depending on a threshold defined by the barrier height. In concert with this is the observation of two distinct hysteresis loops, determined by the initial kinetic energy (incidence angle) of the wave. The results show the inherent versatility of low-index-contrast photonics and hold potential for practical bistable devices, e.g., all-optical switching and optical memory.

Theoretically, the signal wave dynamics can be modeled by a nonlinear Schrödinger equation

$$i\frac{\partial\psi}{\partial z}+\frac{1}{2k_0}\nabla_\perp^2\psi+U\psi+\frac{k_0\Delta n(|\psi|^2)}{n_0}\psi=0, \qquad (1)$$

where $\psi(x, y, z)$ is the slowly varying amplitude of the electric field as it propagates along the z axis, $k_0 = 2\pi n_0/\lambda$ is the wave number for light with wavelength λ/n_0 in a homogeneous medium of refractive index n_0, $U = U(x, y)$ is a refractive index defect, and Δn is a nonlinear index change that depends on the intensity $|\psi|^2$. For example, the standard cubic nonlinear Schrödinger equation results from using the Kerr nonlinearity $\Delta n[I(\boldsymbol{r})] = \varepsilon_2 I$, where ε_2 is the nonlinear coefficient. For the case of photorefractive crystals, as used in the experiment, the nonlinear index change is $\Delta n = -(1/2)n_0^3 r E_{\text{app}}\bar{I}/(1+\bar{I})$, where r is the appropriate electro-optic coefficient with respect to the applied field E_{app} and the crystalline axes and the relative intensity $\bar{I}$ is the input intensity I measured relative to a background (dark current) intensity $I_{\text{background}}$ [8]. For the self-defocusing nonlinearity considered here, there is very little difference in the dynamics between the two cases [9]. Accordingly, we keep the Kerr approximation in the analytics which follow, though we do use the fully saturable case in the numerical modeling. As is well known, Eq. (1) also describes the (macroscopic) ground-state wave function for a fully condensed quantum state, where the wave number k_0 becomes the mass of the underlying particle and the nonlinearity arises from the mean-field contribution of (s-wave) interactions. The results here thus have application to a variety of quantum systems as well, such as superfluids and Bose-Einstein condensates.

It is clear from Eq. (1) that the (optical) wave function can tunnel through a barrier (refractive index) potential, with a rate that is modified by nonlinearity, not only through an interaction-induced correction to the potential energy difference but also through self-phase modifications to the boundary conditions. Even for a single interface, the nonlinearity implies a host of new effects, including multistability [1], splitting solutions for vector beams [10], and enhanced refraction and reflection [2,11]. For double interfaces, i.e., junctions, most work has concentrated on a sequence of linear-nonlinear layers [2–5]. More recently, potential wells fully immersed in the nonlinear medium, with nonlinear-nonlinear boundaries, have been considered [12–17]. However, these studies have been limited to localized wave packets, either by using atomic particles [12,13] or self-focused soliton beams [14–17]. These latter waves are already nonlinear, and the subsequent trapping-ejection dynamics are more akin to a pinning-depinning transition. Further, the presence of self-focusing nonlinearity precludes the use of extended (plane) waves due to modulation instability. Here, we demonstrate

that modified transmission rates can occur with self-defocusing nonlinearity, through a purely repulsive barrier, in the more fundamental case of plane-wave scattering [7].

To gain intuition, we first review the case of an interface between two semi-infinite media of different base dielectric constants $\varepsilon_1 = \varepsilon_0$ and $\varepsilon_2 = \varepsilon_0 + \Delta\varepsilon_l$. For simplicity, we assume that each medium has the same nonlinear response $\Delta\varepsilon_{\rm nl}$. Matching both the wave function and its derivative at the interface gives Snell's law and the Fresnel equations. For a plane wave originally in medium 1, incident on medium 2 at an angle θ_1, Snell's law $(\cos\theta_2/\cos\theta_1)^2 = \varepsilon_1/\varepsilon_2$ becomes [1]

$$(\theta_1 + \theta_2)^2\left(\theta_1^2 - \theta_2^2 + \frac{\Delta\varepsilon_l}{\varepsilon_0} - \frac{\gamma|E_1|^2}{\varepsilon_0}\theta_1^2\right) + 4\frac{\gamma|E_1|^2}{\varepsilon_0}\theta_1^2 = 0, \tag{2}$$

where θ_2 is the refracted angle in medium 2 and it has been assumed that $|\Delta\varepsilon_l + \Delta\varepsilon_{\rm nl}| \ll \varepsilon_0$. For small incident angles θ_1, e.g., near total internal reflection, Fresnel's equations become independent of polarization and yield the transmission and reflection coefficients $t = E_2/E_1 = 2\theta_2/(\theta_1 + \theta_2)$ and $r = (\theta_2 - \theta_1)/(\theta_2 + \theta_1)$, respectively. Using Eq. (2) in this relation gives

$$4(t-1)\theta_1^2 + \left(\frac{\Delta\varepsilon_l}{\varepsilon_o} - \frac{\gamma|E_1|^2}{\varepsilon_0}\theta_1^2\right)t^2 + \frac{\gamma|E_1|^2}{\varepsilon_o}t^4 = 0. \tag{3}$$

This fourth-order equation for transmission can support bistability and hysteresis, with threshold values determined by the strength of the nonlinearity.

For double interfaces, such as the junction shown in Fig. 1(a), one cannot simply cascade the formulas from one interface to the next, since there is nonlinear propagation inside the middle medium. This geometry, commonly used for frustrated total internal reflection [3–5], needs a more careful analysis. Here, we perform numerical simulations on Eq. (1), emphasizing again that, unlike previous studies [1–5], the nonlinearity permeates all three sections of the junction. For simplicity, we fix the angle of incidence (and thus initial kinetic energy) to 1° and the barrier width to be 50 μm and examine the transmission of an incoming plane wave as a function of barrier height and nonlinear self-action [Fig. 1(b)]. Shown is the end result of tunneling, obtained by integrating the total energy transmitted through the barrier. In the linear case, there is the usual transmission for low potentials and total internal reflection for higher barriers, resulting in an exponentially decaying evanescent wave. In the nonlinear case, there are two distinct behaviors, depending on whether the initial incidence angle (beam kinetic energy) is above or below the barrier height. For small barrier heights, linear transport is more efficient, as the self-defocusing nonlinearity (repulsive interaction) creates an enhanced pressure upon reflection. For stronger potentials, at and above the classical transition point when the effective potential equals the initial kinetic energy, nonlinearity suppresses the evanescent decay. In this regime, the nonlinearity serves to index match the incident wave with the defect, while the self-repellant force of the tunneled light encourages further transport across the barrier. Paradoxically, this nonlinear effect is enhanced for narrower and higher barrier potentials [7], as the nonlinear pressure within the sandwich layer becomes more pronounced.

Experimentally, we observe these dynamics by considering plane-wave scattering in a self-defocusing photorefractive crystal. Defect and signal beams are created by splitting cw light from a 532 nm laser and then imaging each individually onto an 8 $\rm mm^3$ SBN:60 ($Sr_{0.6}Ba_{0.4}Nb_2O_6$) crystal. The defect is created by optically inducing an antiwaveguide in the medium [18,19]. To do this, a relatively broad (200 μm) beam of ordinarily polarized light is focused onto the crystal using a cylindrical lens; the width and polarization ensure near-diffractionless propagation over the length of the crystal, while the self-defocusing nonlinearity causes the bright induction beam to locally lower the refractive index. Changing the intensity of this writing beam allows control of the index change (barrier height). An extraordinarily polarized plane wave is then sent at an angle across this defect. The output intensity is imaged into a CCD camera.

Experimental results of transmission across the defect are shown in Fig. 1(c). As in the simulations [Fig. 1(b)], there is a clear crossover behavior when the barrier height equals the incident kinetic energy. Moreover, since the tunneling is nonlinear, there is a bistability in the transmission. To observe this, we keep the incident angle fixed at 1.5° and change the intensity of the plane wave (thus changing its self-energy). As shown in Fig. 2, the two separate energy regions have two different hysteresis loops. For incidence energies above the barrier height ($\Delta n/n_0 \sim 2 \times 10^{-4}$), nonlinearity serves to decrease transmission, and the hysteresis loop goes clockwise

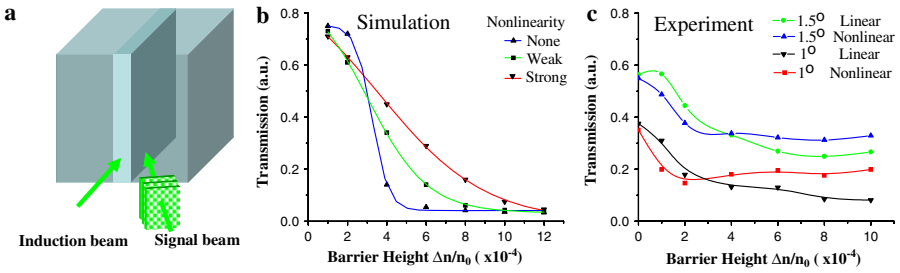

FIG. 1 (color online). Wave tunneling through a small barrier potential. (a) Experimental scheme illustrating a plane wave incident upon an optically induced refractive index barrier. (b) Numerical simulation of transmission through the junction. (c) Experimental results.

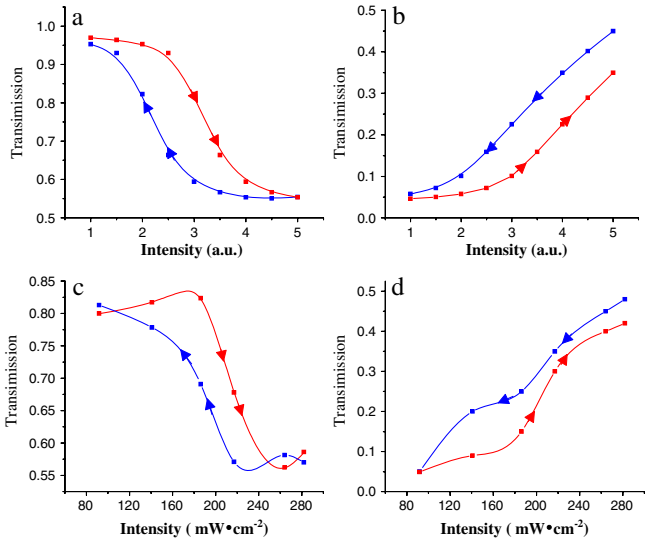

FIG. 2 (color online). Optical hysteresis effects of wave tunneling through a barrier potential. Top row is numerical output and bottom row is experimental output for an incidence angle of 1.5°. (a),(c) For a small barrier ($\Delta n/n_0 = 2 \times 10^{-4}$), the transmission spectrum exhibits clockwise loops. (b),(d) For a high barrier ($\Delta n/n_0 = 6 \times 10^{-4}$), the tunneling spectrum exhibits counterclockwise loops.

[Figs. 2(a) and 2(b)]. For the opposite case, for incidence energies below the barrier height ($\Delta n/n_0 \sim 6 \times 10^{-4}$), nonlinearity enhances transmission, and the loop runs counterclockwise [Figs. 2(c) and 2(d)]. For this latter hysteresis curve, our numerical results suggest the required index change to complete the loop in the upper end is $\Delta n/n_0 \sim 10^{-3}$, which is beyond our crystal's physical limit of $\Delta n/n_0 \sim 10^{-4}$. To our knowledge, the two separate and reversed hysteresis trends have not been reported before, in any physical system.

While Eq. (2) gives the transmission and reflection coefficients on either side of an interface, it does not say anything about the subsequent nonlinear evolution of the waves. To examine this, it is useful to rewrite the original Schrödinger equation (1) using the polar (Madelung [20]) transformation $\psi(x, z) = \sqrt{\rho(x, z)}\exp[iS(x, z)]$

$$\frac{\partial \rho}{\partial z} + \nabla_\perp(\rho \nu) = 0, \tag{4}$$

$$\frac{\partial \nu}{\partial z} + \nu \nabla_\perp \nu = \nabla_\perp \Delta n(\rho) + \nabla_\perp U + \nabla_\perp\left(\frac{1}{2\sqrt{\rho}} \nabla_\perp^2 \sqrt{\rho}\right). \tag{5}$$

These equations describe the optical dynamics in terms of ideal, Euler-like fluid flow, where $\nu = \nabla_\perp S$ is an effective flow velocity and $\Delta n(\rho)$ can be interpreted as an optical pressure (positive for defocusing nonlinearity). The last term in Eq. (5), known as the "quantum pressure" in condensed matter systems, is a third-order restorative term resulting from diffraction. It characterizes spatial dispersion and prevents discontinuities in the wave function, e.g., near the interfaces and at the steep gradients arising from the convective derivatives. For example, the competition between wave steepening and diffractive regularization can result in spatial dispersive shock waves [9,21].

The observation of shock waves is facilitated by having a constant, low-level background, so that phase differences from the nonlinearity appear as intensity variations [9,22]. This setup is different than the traditional transmission-reflection geometry used above, in which a plane wave is incident from the right side of the barrier and there is no initial field on the left side. However, there are many physical situations in which there is field everywhere, e.g., a (super)fluid passing over and through a small obstacle [23]. In this case, there can be significant dynamics on the transmission side of the barrier as well, as the transmitted field now has a background with which it can interact.

Tunneling dynamics with initial field everywhere are shown numerically in Fig. 3. In the linear case [Fig. 3(a)], there are interference fringes formed near the interfaces as phase accrues through transmission and reflection, but no evolution in the wave fronts themselves. By contrast, in the nonlinear case, energy is transported farther away from the interfaces, creating a distributed profile with much lower peak intensities, and there is significant evolution dynamics. Both the reflected and transmitted waves self-steepen as they propagate, eventually breaking into right- and left-going dispersive shock waves [9]. These are the phase jumps and dark soliton trains predicted for nonlinear tunneling in a superfluid [7]. Note especially that such shock

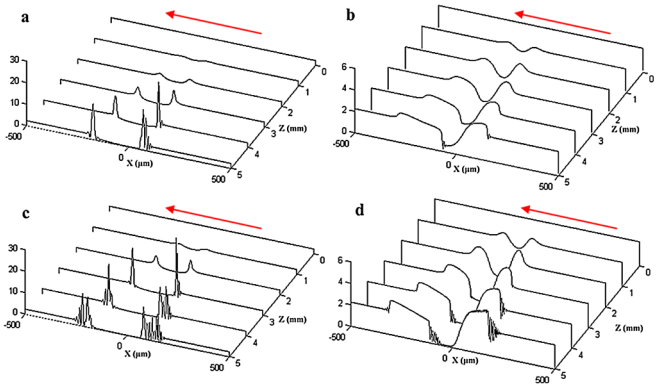

FIG. 3 (color online). Numerical simulation of full-field tunneling through a barrier. Plane-wave incidence onto a barrier centered at $X = 0$ with FWHM ~ 100 μm (a),(c) Linear case. (b),(d) Nonlinear case. Note the difference in scale. Shown are output pictures for (a),(b) weak ($\Delta n/n_0 = 2 \times 10^{-4}$) and (c),(d) strong ($\Delta n/n_0 = 6 \times 10^{-4}$) barrier heights.

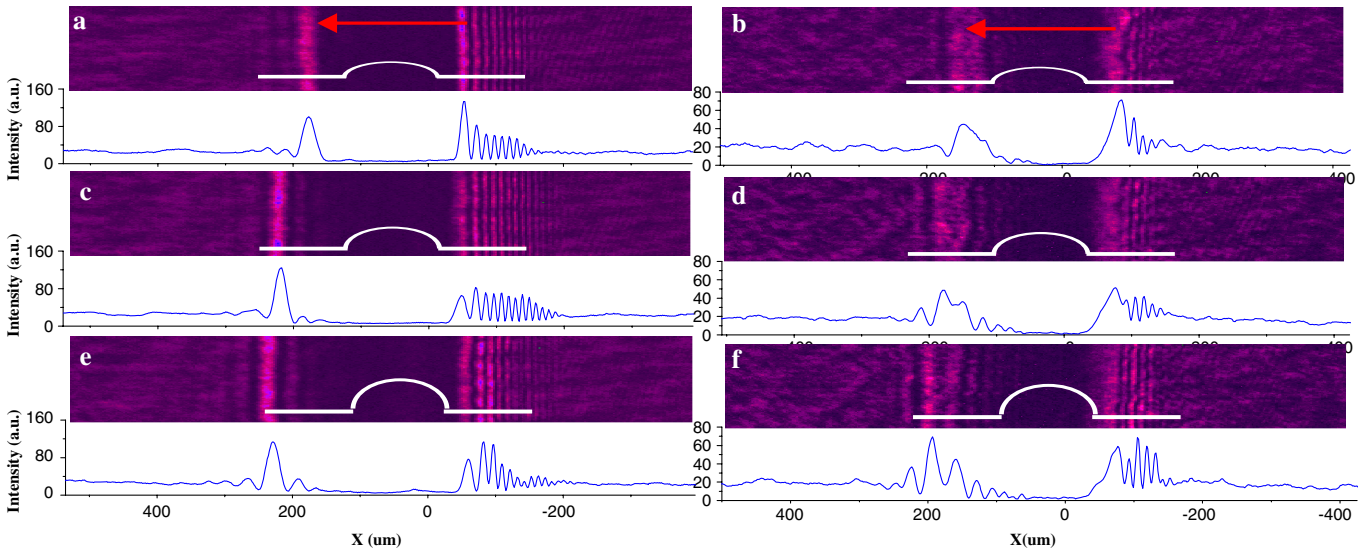

FIG. 4 (color online). Experimental observation of full-field tunneling through a barrier. Left column: Linear case; right column: nolinear case. Shown are output pictures for (a),(b) weak ($\Delta n/n_0 = 2 \times 10^{-4}$), (c),(d) medium ($\Delta n/n_0 = 4 \times 10^{-4}$), and (e),(f) strong ($\Delta n/n_0 = 6 \times 10^{-4}$) barrier heights. In all cases, the input angle was 1°.

waves appear in the shadow region behind the defect as well. Here, the darkness of the shadow implies a higher refractive index (the medium is defocusing), drawing a backflow towards the barrier and further encouraging the tunneling of light through it. This counterpropagating flow, caused here by the imposed defect, is also predicted to occur self-consistently around vacuum (zero-intensity) points in dispersive shock waves [24]. From the rest frame of the angled wave, the barrier is being dragged through it. There is now a (dispersive) bow shock created at the front of the obstacle, while the dynamics behind the barrier is the optical version of a (1D) fluid wake.

Experimental examples of this full-wave behavior are shown in Fig. 4. In the linear case, there are interference fringes upon reflection and transmission, with the highest intensity peaks appearing at the barrier edges. In the nonlinear case, these peaks propagate faster, appearing a significant distance from the junction walls. The light falloff at the interfaces is also more gradual than in the linear case, since tunneling and backflow are enhanced. As predicted [7], dark solitons in the fluid wake appear only if the barrier height exceeds a threshold value ($\sim 2 \times 10^{-4}$) for a given incident velocity. These nonlinear effects become more pronounced as the barrier height is increased.

In conclusion, we have shown, theoretically and experimentally, that transmission through a small barrier potential can be greatly altered by nonlinearity. Bistability was observed and, depending on the relative incidence energy, the corresponding hysteresis loops would run clockwise or counterclockwise with intensity. Phase singularities were found on reflection and transmission, seeding the formation of dark solitons and dispersive shock waves. The results were demonstrated for optical tunneling through a small refractive index defect but will hold for any Schrödinger system that contains a nonlinear junction.

[1] A. E. Kaplan, JETP Lett. **24**, 114 (1976).
[2] P. W. Smith and W. J. Tomlinson, IEEE J. Quantum Electron. **20**, 30 (1984).
[3] B. Bosacchi and L. M. Narducci, Opt. Lett. **8**, 324 (1983).
[4] T. Peschel *et al.*, J. Opt. Soc. Am. B **5**, 29 (1988).
[5] G. I. Stegeman *et al.*, J. Lightwave Technol. **6**, 953 (1988).
[6] A. C. Newell, J. Math. Phys. (N.Y.) **19**, 1126 (1978).
[7] V. Hakim, Phys. Rev. E **55**, 2835 (1997).
[8] N. V. Kukhtarev, V. B. Markov, S. G. Odulov, M. S. Soskin, and V. L. Vinetskii, Ferroelectrics **22**, 949 (1979).
[9] W. Wan, S. Jia, and J. W. Fleischer, Nature Phys. **3**, 46 (2007).
[10] F. W. Ye, Y. V. Kartashov, and L. Torner, Opt. Lett. **32**, 394 (2007).
[11] M. Peccianti *et al.*, Nature Phys. **2**, 737 (2006).
[12] M. Albiez *et al.*, Phys. Rev. Lett. **95**, 010402 (2005).
[13] S. Folling *et al.*, Nature (London) **448**, 1029 (2007).
[14] Y. Linzon *et al.*, Phys. Rev. Lett. **99**, 133901 (2007).
[15] G. Dekel *et al.*, Phys. Rev. A **75**, 043617 (2007).
[16] A. Barak *et al.*, Phys. Rev. Lett. **100**, 153901 (2008).
[17] M. Peccianti *et al.*, Phys. Rev. Lett. **101**, 153902 (2008).
[18] N. K. Efremidis *et al.*, Phys. Rev. E **66**, 046602 (2002).
[19] J. W. Fleischer *et al.*, Phys. Rev. Lett. **90**, 023902 (2003).
[20] E. Madelung, Z. Phys. **40**, 322 (1927).
[21] N. Ghofraniha *et al.*, Phys. Rev. Lett. **99**, 043903 (2007).
[22] S. Jia, W. Wan, and J. W. Fleischer, Phys. Rev. Lett. **99**, 223901 (2007).
[23] P. Engels and C. Atherton, Phys. Rev. Lett. **99**, 160405 (2007).
[24] G. A. El, V. V. Geogjaev, A. V. Gurevich, and A. L. Krylov, Physica (Amsterdam) **87D**, 186 (1995).